ENGINEERING RESEARCH INSTITUTE
UNIVERSITY OF MICHIGAN
ANN ARBOR

FINAL REPORT

ANTI-ICING AND ANTI-FROSTING OF AERIAL PHOTOGRAPHIC WINDOWS

M. P. MOYLE
R. E. CULLEN

Project 2197

WRIGHT-PATTERSON AIR FORCE BASE
WRIGHT AIR DEVELOPMENT CENTER
CONTRACT NO. AF 33(616) 2268

October, 1954

SUMMARY

This report summarizes the work done under Air Force Contract AF 33(616)-2268 on anti-icing and anti-fogging studies and services. A literature survey of subjects related to the anti-fogging and anti-frosting problem constituted the initial phase of the project. The second phase consisted of the following studies:

a. thermal boundary layer as an optical wedge,

b. thermodynamic evaluation of the installation of electrically conductive windows in the McDonnell RF-101, and

c. interferometric evaluation of the electrically conductive windows used in the RF-101.

TABLE OF CONTENTS

LIST OF ILLUSTRATIONS

NOMENCLATURE

b	Free stream fringe width
L	Length of medium through which light traverses
M	Mach number nondimensional
n	Refractive index in first medium
n'	Refractive index in second medium
ΔN	Fringe shift measured in multiples of free-stream fringe width
R_{ex}	Reynolds number $\left(\frac{DV\rho}{\mu}\right)$, nondimensional
t'	Time for light beam to pass through length L at velocity V'
T	Reference temperature, °R
T'	Measured temperature, °R
ΔT	Temperature change
V	Velocity of light through medium with refractive index n
V'	Velocity of light through medium with refractive index n'
x	Distance, feet
y	Distance into boundary layer measured perpendicular to window surface, feet
α	Wedge angle, seconds
β	Angle ray makes with perpendicular to surface
δ	Deflection of light ray, seconds
Θ	Temperature difference
λ_o	Wave length of light in vacuum
λ	Wave length of light in media of refractive index n
λ'	Wave length of light in media of refractive index n'
μ	Vicosity, pounds per foot second
ρ	Density in media of refractive index n, pounds per cubic foot

ρ' Density in media of refractive index n', pounds per cubic foot

ϕ Angle bent ray makes with perpendicular, seconds

Ω Temperature rise, temperature at station one - temperature at wall, °R

SUBSCRIPTS

i Incident ray

H Hydrodynamic boundary layer

n Station

t Thermal boundary layer

y Characteristic at distance from window surface, ft

ANTI-ICING AND ANTI-FROSTING OF AERIAL PHOTOGRAPHIC WINDOWS

1. INTRODUCTION

Present day aerial photographic missions operate under conditions where fog and/or frost formations would occur on the photographic windows if some means of protection were not provided. Many fog and frost prevention systems have been proposed and evaluated in the past decade. Among these are the forced hot air system, infrared radiation, dehumidified camera hood, dielectric heating, and electrically conductive surface films. The forced hot air system has found the widest application to date, despite its bulk. Recent developments with electrically conductive films show considerable promise that this method of heat application may solve much of the defogging and defrosting problem.

In this connection, the University of Michigan has undertaken the task of providing studies and services for anti-fogging and anti-frosting of photographic windows under contract AF 33(616)-2268 with the Air Force. The initial phase of this contract consisted of a literature survey of the fields related to the anti-fogging and anti-frosting problem and was of approximately four-months duration. A report which included a bibliography on topics related to the anti-fogging and anti-frosting problem and a discussion of present and future problems in aerial photography was issued.[8] Another reference* which described the work done in the field of aerial photography during and after World War II under the direction of NDRC has been reviewed recently. The work described covers a considerable portion of the field of aerial photography. Under NDRC lenses of high resolution, anti-vibration camera mounts, shutters, and various other associated photographic equipment were developed. In conjunction with this development work, a flight-testing program was carried out to compare in-flight results with laboratory results and to determine which element in the photographic system contributed most to the loss of resolution. In general, it was found that in-flight results were considerably inferior i.e., much lower resolution, to laboratory results. This has become a generally accepted fact. Many of the factors thought to cause serious loss of resolution were found to be essentially unimportant. Vibration was found to be one of the major causes for loss of resolution in flight.

*Not available during the literature survey.

2. DIFFRACTION THROUGH A THERMAL BOUNDARY LAYER AS A SOURCE OF LOSS OF RESULTION

During the initial studies, a question arose concerning the effect of velocity fluctuations in a hot air jet on resolution. After some preliminary investigation, the problem was reduced to the effect of a thermal boundary layer on a light ray. This problem was examined because most of the anti-fogging and anti-frosting systems are of the thermal type and will necessarily have a thermal boundary layer associated with them. Guided missiles, anticipated as future photo-reconnaissance tools, will also have a hydrodynamic boundary layer created by skin friction at high-flight speeds. The thermal boundary layer is a thin layer of air across which the change from surface temperature to free-stream temperature occurs. The thermal boundary layer begins at the leading edge of the heated surface and increases in thickness as it progresses downstream. Since the thickness of the boundary layer increases, it should act as an optical wedge. The magnitude of the optical wedge effect was the subject of this investigation.

METHOD OF ANALYSIS

Although there might be either a laminar or turbulent boundary layer, or even a region of separation over the window in an actual situation, the case of a laminar boundary layer was chosen for preliminary study. The hydrodynamic boundary layer thickness was estimated by the simplified formula given by Eckert [3]

$$\delta_H = \frac{4.64}{\sqrt{Rex}} \qquad (1)$$

for a specified condition*, the thermal boundary layer thickness was estimated to be of the same order of magnitude.

The temperature distribution through the boundary layer was calculated at sixteen points using the parabolic distribution given by Eckert[3] as

$$\frac{\Omega}{\Theta} = \frac{3}{2}\left(\frac{y}{\delta_t}\right) - \frac{1}{2}\left(\frac{y}{\delta_t}\right)^3 , \qquad (2)$$

(the temperature profile is shown in Fig. 4). The refractive index of air was then calculated at these same points through the boudary layer using the law of Dale and Gladstone[2]. The value of n_o was taken as the average

*Sample computation is included in Appendix 1.

value for light between 0.431 and 0.759 microns as given by Jakob[5]. A tabulation of the temperature, refractive index, and refractive index ratios at various points through the boundary layer is shown in Table I.

TABLE I

TEMPERATURE, REFRACTIVE INDEX, REFRACTIVE INDEX RATIO, AND WEDGE ANGLE AT VARIOUS POINTS THROUGH THE BOUNDARY LAYER

y	T_y	N_y	$\mu = \frac{n_{y_1}}{n_{y_2}}$	α
0	510.0	1.000052739	0.999999520	120
.0001	505.4	1.000053219	0.999999511	160
.0002	500.8	1.000053708	0.999999502	200
.0003	496.2	1.000054206	0.999999010	200
.0005	487.3	1.000055196	0.999999450	140
.0006	482.5	1.000055745	0.999999475	100
.0007	478.0	1.000056270	0.999999477	120
.0008	473.6	1.000056793	0.9999998937	100
.0010	464.9	1.000057856	0.9999998923	80
.0012	456.4	1.000058933	0.9999998422	60
.0015	444.5	1.000060511	0.9999998408	41
.0018	433.1	1.000062103	0.9999998979	41
.0020	426.1	1.000063124	0.9999998545	60
.0025	416.5	1.000064579	0.9999997471	60
.0030	400.8	1.000067108	0.999999152	41
.0035	395.8	1.000067956	0.999999516	41
.0038	393.0	1.000068440	1.000000000	41

By Snell's law[4] (reference to Fig. 1), $n \sin \beta = n' \sin \phi$. Thus, a light ray passing from a zone of air of refractive index n to one of refractive index n' is bent from its original path.

Although the temperature and thus refractive index varies continuously throughout the boundary layer, the variation is approximately linear over short distances, therefore a stepwise calculation using the average over the step yields a very good approximation provided sufficient steps are taken. (No analytical solution could be found for the differential equation describing the system.) Sixteen steps, each assumed to be at the average temperature across the step, were chosen for this calculation. The first step simply involves the application of Snell's law.

In order to proceed with the calculation beyond the first step, it is necessary to know the angle that the bent ray from the first step makes with the perpendicular to the second step; or, in general, the angle that the bent ray from the n^{th} step makes with the perpendicular to the $(n+1)^{st}$ step. Reference to Fig. 2 shows that

$$\begin{aligned}
\beta_i &= \angle EDF \\
\beta_1 &= \angle GDH \\
\phi_1 &= \angle DHI \\
\alpha_1 &= \angle BAC = \angle DJI \\
\delta &= \angle KDH \\
JI &\perp AC \\
FJ &\perp AB \\
\phi_1 &= \angle ADB - (\angle ADB - \beta_1) - (\angle AIH) \\
&\quad 180 - (90 - \beta_1) - (90 - \alpha_1) = \beta_1 + \alpha_1 ,
\end{aligned}$$

or, in general,

$$\phi_n = \beta_n + \alpha_n .$$

Reference to Fig. 3 yields

$$\begin{aligned}
\angle BED &= 180 - \phi_n \\
\angle DFA &= \beta_1 \\
\angle FAD &= 180 - \beta_i - \alpha_t \\
\angle BAE &= 180 - (180 - \beta_i - \alpha_t) \\
\angle ABE &= 180 - [180 - (180 - \beta_i - \alpha_t)] - [180 - \phi_n] \\
&\quad 18/0 ,
\end{aligned}$$

or

$$\delta = \angle ABC = \phi_n - (\beta_i + \alpha_t) .$$

Where δ is the total angle the incident ray deviates from its original path after passing through the thermal boundary layer.

The optical path was computed stepwise through the boundary layer and the deviation δ was plotted as a function of the angle of incidence of the original ray; Fig. 5.

Figure 5 shows that for the specific case examined, the thermal boundary layer acts as an optical wedge; the magnitude of which depends on the angle of incidence. Thus wide-angle mapping lenses might be subject to wedge errors of the order of magnitude of the limits of error of the windows themselves.

Since these calculations were intended to be of an exploratory nature only, complete evaluation of the optical distortion caused by the laminar-thermal boundary layer over a range of conditions cannot be accomplished at this time.

When the boundary layer becomes turbulent, the analysis becomes more complicated. The turbulent boundary layer is considered to consist of three zones, i.e., a laminar sublayer next to the wall, a transition zone, and an outer turbulent layer. Although it is possible to calculate a temperature distribution through the turbulent layer, it is only possible to evaluate statistically the effects the turbulent eddies in the outer zone will have on the light path. Sharp temperature and thus sharp refractive index gradients, which are continuously changing might well be the major cause of distortion in a turbulent flow with the overall temperature drop having a secondary effect*.

In the case of a plane jet discharging hot air across the interior surface of the window, the temperature distribution is quite complicated. The total temperature drop is divided among the outer thermal boundary layer, the window glass, and the jet stream itself. The temperature increases through the jet from cabin temperature to the maximum jet temperature, then decreases to the temperature of the interior surface of the window. The temperature then drops in a linear manner through the window (for the steady case) and finally drops to the free-stream temperature across the outer thermal boundary layer; according to the previous discussion.

Considerable optical distortion is anticipated from a jet stream in view of this torturous optical path even under conditions of steady flow. Air velocities from blowers and jets currently being used generally fluctuate considerably (a constant pressure reservoir might be employed to

*Since this work was completed, a report by Liepmann[6] has been made available to the writer. Liepmann examined the simple case of a laminar boundary layer considered parallel to the surface and concludes that for this case, the details of the flow inside the boundary layer are unimportant; that is, Snell's law can simply be applied from the point of initial refractive index to the point of final refractive index. A comparison of the results for the specific case examined in this paper with those of Liepmann indicates that a considerable increase in wedge angle results when the growth of the boundary layer is considered. Further comparison with Liepmann's results indicates that the case examined in this paper is a very mild one; that is, considerably higher deflections are possible as the temperature drop is increased and the altitude is decreased. Liepmann then goes on to examine the turbulent boundary layer, again considered parallel to the surface and consisting of one turbulent zone. Turbulent density fluctuations were studied on the basis of geometrical optics. A crude estimate of the diffusion of a ray for a typical case, Mach 2 at sea level, was found to be approximately 82 seconds of arc.

overcome this), and thus, the temperature profile through a jet stream will be continually shifting. A temperature fluctuation through the jet stream will create temperature fluctuations through the window and outer boundary layer in planes both normal and parallel to the direction of flow. Each of these temperature fluctuations will probably have adverse effects on the optical resolution realized in the photographic product.

As flight speeds increase into the supersonic, the effect of aerodynamic heating will become pronounced. If photo reconnaissance or telecasting operations being carried out from guided missiles traveling at velocities approaching Mach 2 are envisaged, then window surface temperatures of the order of 250°F would be experienced. Thus injection of cold air into the boundary layer might be necessary to cool the photographic windows. Here again the effects of turbulence and mixing are unknown. Shock waves will also be present in transonic and supersonic flight. Sharp density gradients occur across these shocks; and therefore, can be expected to constitute wedges of considerable magnitude, depending on the obliquity of the shock. These problems of aerodynamic heating and shock-wave interaction may well be experienced at present in photographic studies of models in supersonic wind tunnels.

The analysis of light deviation caused by thermal boundary layers should be extended over a wider range using more rigorous methods of analysis which take into account the effect of variable fluid properties. Experimental investigations should be carried out to determine the magnitude of optical deviations caused by both laminar and turbulent boundary layers, as well as shock waves. Experimental studies should also be made on optical deviations caused by velocity fluctuations in plane jets.

3. EVALUATION OF ANTI-FROSTING SYSTEM FOR THE McDONNELL RF-101

Although more work of the nature described above was anticipated at the time the above analysis was made, time did not permit. The Air Force requested that this laboratory give priority to a thermodynamic study of the application of the electrically conductive windows planned for the McDonnell RF-101. The project was initiated in June, 1954, and consumed most the remaining contract period. Conferences were held with Air Force and McDonnell personnel concerning the performance requirements of the anti-fogging, anti-frosting system. Preliminary studies[7] indicated that the performance requirements chosen were unrealistic and were modified accordingly. Steady-state heat requirements for the new condition were calculated for a pressure altitude of 50,000 feet as a function of Mach number. The results indicated that sufficient power was available for

the anti-fogging application. Transient studies* were then made for a specified dive to near sea level. It was concluded that the system would be entirely adequate for fog prevention on both inner and outer surfaces if the inner surface were maintained at 85°F before entering into the dive and a constant heat flux equal to the steady-state heat requirements at 50,000 feet were supplied during the dive. It was further concluded that icing protection would be marginal, especially with the conductive film on the inner surface of the window. It was pointed out that the above conclusions were valid for the specified flight plan and rate of descent, but might be altogether different if the flight plan or rate of descent were appreciably altered.

4. INTERFEROMETRIC STUDIES OF ELECTRICALLY CONDUCTIVE PHOTOGRAPHIC WINDOWS

The final study undertaken during the contract year was the evaluation of the type of photographic windows being installed in the McDonnell RF-101. Two 8 inch by 8 inch photographic windows coated with the Liberty 81E electrically conductive coating were supplied to this laboratory by the Libbey-Owens Ford Company for use in experimental work. The Liberty 81E coating has been described as a thin layer of gold (order of 10 microns) between a sandwich of magnesium flouride[1,2]. Preliminary tests were run on one of the windows to obtain information concerning the power limits, etc., before installation in a wind tunnel. The window was tested by immersion in a bath of tap water maintained at 85°F while increasing the power loading at 15 minute intervals. Failure occurred at 1080 watts per square foot. A conference was held at Wright Field on September 20, 1954, concerning the windows, since Air Force personnel had also experienced several window failures during testing. Libbey-Owens Ford representatives suggested that the specimen tested by this laboratory had failed because of galvanic action and that specimens tested at Wright Field had failed due to surface swatches. The general conclusions were that the hardness of the outer protective film should be improved.

*This laboratory felt that fogging or frosting could occur on either surface of the windows during a transient dive if conditions were such that the driving force for mass transfer were toward the window. A recent report by NACA[1] shows that frosting can occur at Mach 1.3, if conditions of humidity and temperature are favorable.

The optical quality and temperature distribution across the remaining 8 inch by 8 inch photographic window received by this laboratory were examined using the University of Michigan Mach-Zehnder interferometer. The principle of operation of the Mach-Zehnder interferometer is based on the pheomena of light interference and the change of refractive index of light with the density of the medium through which it passes. In Fig. 6 a beam of collimated light is divided by a half-silvered plane mirror, M_1. The two resulting beams of light travel different paths of exactly the same length in the instrument and are recombined by another half-silvered mirror, M_3, and fall on screen, P. If the optical arrangment is aligned perfectly, the light falling on P will be in phase and uniform illumination will result. If, however, a mirror is rotated slightly about an axis parallel to the page, the optical path of one beam is slightly longer than the optical path of the other. The light falling on screen P then is out of phase; the waves differing by an odd number of half wavelengths canceling each other and the waves differing by an even number of half wavelengths reinforcing each other. The result is the so-called "fringe" pattern consisting of light and dark bands evenly spaced. By varying the position of the mirror very precisely, any desired spacing of the fringes can be obtained. Now, if a density disturbance is placed at the test section S, the resulting pattern of the fringe lines on the screen can be observed. The distance a fringe line is deviated at a point, then is a direct measure of the density of the media at that point.

A short explanation of the evaluation of the density by the fringe shift method will be given.

From the Gladstone-Dale relation,

$$n-1 = \text{const}\ \rho, \tag{3}$$

where n is the index of refraction and ρ is the density. Therefore,

$$\frac{n-1}{\rho} = \frac{n'-1}{\rho}, \tag{4}$$

or

$$n'-n = (n-1)\left(\frac{\rho'}{\rho}-1\right). \tag{5}$$

If a light beam traverses a medium of length L of index of refraction n', wave length λ, with a velocity V', the time for light to pass through L is

$$t' = \frac{L}{V'}. \tag{6}$$

In the same time a beam of light of velocity V will transverse a distance L + x so that

$$\frac{L}{V'} = \frac{L+x}{V} \quad , \tag{7}$$

but

$$\frac{V}{V'} = \frac{\lambda}{\lambda'} \quad . \tag{8}$$

therefore,

$$\frac{L}{\lambda'} = \frac{L+x}{\lambda} \quad , \tag{9}$$

and

$$x = \frac{L(\lambda-\lambda')}{\lambda'} \quad . \tag{10}$$

By definition, $\frac{\text{Velocity of Light in Vaccum}}{\text{Velocity of Light in Medium of Index n}} = n = \frac{\lambda_o}{\lambda}$

λ_o = Wave Length in Vacuum.

Therefore,

$$n = \frac{\lambda_o}{\lambda} \; ; \quad n' = \frac{\lambda_o}{\lambda'} \quad .$$

Substituting in Equation 10

$$x = \frac{L}{n}(n'-n) \quad , \tag{11}$$

$$x = L\left(\frac{\lambda}{\lambda_o}\right)(n'-n) \quad , \tag{12}$$

$$\frac{x}{\lambda} = \frac{L}{\lambda_o}(n'-n) \quad . \tag{13}$$

Now, let ΔN be the fringe shift measured in multiples of free-stream fringe width b, then

$$\Delta N = \frac{Y}{b} \quad ,$$

Where Y is the total distance the fringe is shifted. Since the fringe shift gives a measure of the number of wavelengths,

$$\Delta N = \frac{Y}{b} = \frac{x}{\lambda} \quad . \tag{14}$$

Therefore, substituting in Equation 13,

$$\frac{Y}{b} = \frac{L}{\lambda_o}(n'-n) \tag{15}$$

and finally, substituting the value of n'-n in Equation 5 into Equation 15, the following is obtained

$$\Delta N = \frac{Y}{b} \quad \frac{L}{\lambda_o}(n-1)\left(\frac{\rho'}{\rho}-1\right) \quad . \tag{16}$$

Using the perfect gas law and changing signs in Equation 15 by assuming that the measured temperature T' is greater than the reference temperature T,

$$\Delta N = \frac{n-1}{\lambda_o} \quad \frac{T'-T}{T'} \quad ; \tag{17}$$

solving explicitly for ΔT,

$$\Delta T = T'-T = T\frac{\Delta N}{(n-1)\frac{L}{\lambda_o} - \Delta N} \quad . \tag{18}$$

By means of Equation 16 the density distribution in the flow can be calculated. If it is assumed that the pressure does not vary throughout the region studied, as is the case for the pressure normal to the surface of an airfoil in the boundary layer, or in free convection studies, then the temperature distribution can be determined by Equation 18.

The results of the interferometric study are shown in Fig. 7 and 8. Figure 7a shows the interferometric pattern for the undeviated field before turning on the power. The wide vertical dark band near the center of the picture is the edge of the photographic window being studied. The narrow irregular band coming off at an angle is the power lead attached to the bus bar which appears as the little triangular bulge at the top of the window. The alternate horizontal light and dark bands are the interferometric fringes. In some of the pictures, a narrow vertical line appears about an inch from the glass plate. This was a plumb line used for aligning the plate with the vertical.

Since the window was at room temperature, the fringe lines are perpendicular to the surface of the window. In Fig. 7b and 7c however, the fringes bend up sharply as the plate is approached, due to the rise in temperature in the vicinity of the window. The maximum temperature reached was approximately 125°F in Fig. 7c. The field over the window appears quite uniform except in the vicinity of the bus bar where the dark bands curve back on themselves; indicating a cooler surface. This effect persists for

a distance about one inch from the edge of the bus bar. This effect will be even greater when the window is set in an unheated frame, thus thermostatic control elements should be located accordingly.

The optical quality of the glass was examined by placing a photographic window in each leg of the interferometer, i.e., the test section and the compensating section, and noting the fringe pattern. If very poor windows were used, no fringes could be developed. High-quality glass would be represented by alternate parallel light and dark bands. Imperfections would be indicated by deviations from parallelism or by bending. Pictures were taken with the test specimen both unheated and heated. Figure 8a shows the fringes for the unheated window used in the test section. At the top of the picture the alternate light and dark bands represent the fringes in free air. The light gray band directly below represents one pane of window glass, while the narrow dark band represents the bus bar on the second pane of glass. Below the bus bar are the fringes developed after passing the light through the two pieces of glass specimens; one in the test section, the other in the compensating section. The fringes are quite parallel in both the unheated (Fig. 8b) and heated runs (Fig. 8c). Very slight irregularities are noted by the waviness of the fringes; however, the optical quality is in general excellent. Again, deviations are noted near the bus bar for the heated run (Fig. 8c) which shows the surface curvature developed due to the lower temperature near the bus bar.

APPENDIX I

EXAMPLE CALCULATION FOR LIGHT DEVIATION THROUGH BOUNDARY LAYER

ASSUMPTIONS

(1) Laminar Flow over Window
(2) Hydrodynamic and Thermal Boundary Layers Begin at Edge of Window
(3) Refractive Index Varies with Temperature According to Law of Gladstone and Dale

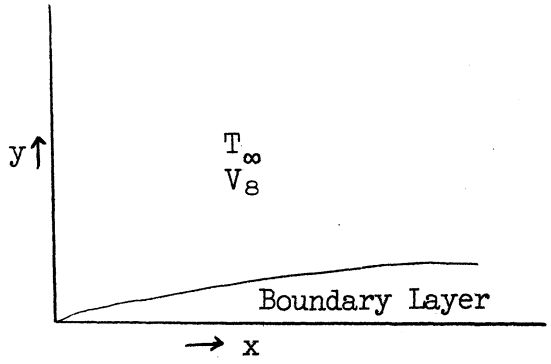

FREE-STREAM CONDITIONS

$U_\infty = 100$ ft/sec
$T_\infty = -67°F$
$T_s = 40°F$

(A) Hydrodynamic Boundary Layer Thickness at x = 1/2 ft

$$\delta_H = \frac{4.64x}{\sqrt{Re}} = \frac{4.64 \times 0.5}{610} = 0.0038 \text{ ft}$$

$$\delta_t = \delta_H \frac{1}{Pr^{\frac{1}{3}}} = \delta_H \text{ (assume } Pr^{\frac{1}{3}} \approx 1.0)$$

(B) Temperature Distribution

$$\frac{T_y - T_s}{T_\infty - T_s} = 1.5\left(\frac{y}{\delta_t}\right) - 0.5\left(\frac{y}{\delta_t}\right)^3$$

Calculation of optical deviation at 30° angle of incidence,

Step 1

$$\beta_i = 30°$$

$$\beta_1 = \text{arc sin}\left(\frac{\sin 30}{.99999952}\right) = 30°0'.057"$$

$$\phi_1 = \beta_1 + \alpha_1$$

$$= 30°0'.057" + 41" = 30°0'41.057" .$$

Step 2

$$\beta_2 = \text{arc sin}\left(\frac{\sin 30°41.057"}{.9999991}\right)$$

$$\sin 30°41" = .500172713$$

$$41.057 = 237$$

$$42 = .50017633$$

$$\beta_2 = \text{arc sin}\left(\frac{.50017237}{.99999915}\right) = \text{arc sin}\,(.50017280)$$

$$.50017213 = \sin 30°41"$$

$$.50017280 = \sin x$$

$$.50017633 = \sin 30°42" ,$$

then,

$$\beta_2 = 30°0'41.160"$$

$$\phi_2 = \beta_2 + \alpha_2$$

$$= 30°41.160" + 41" = 30°1'22.160"$$

$$\beta_4 = \text{arc sin}\,\frac{(\sin \phi_3}{\mu_3)}$$

$$\beta_{16} = \text{arc sin}\left(\frac{\sin 30°24'5.804"}{.99999952}\right)$$

$$\sin 30°24'5.804" = .50605803 ,$$

then

$$\beta_{16} = \arcsin\left(\frac{.50605803}{.99999952}\right)$$

$$= \arcsin(.50605827) \quad ,$$

or

$$\beta_{16} = 30°24'5.861"$$

$$\phi_{16} = \beta_{16} + \alpha_{16}$$

$$= 30°24'5.864" + 120" = 30°26'5.861"$$

$$\delta = \phi_{16} - \theta_1 - \alpha_t$$

$$= 30°26'5.861" - 30°26'4.0"$$

$$= 1.861" \quad .$$

BIBLIOGRAPHY

1. Coles, W. D. and Ruggeri, R. S., "Experimental Investigation of Sublimation of Ice at Subsonic and Supersonic Speeds and Its Relation to Heat Transfer", NACA TN3104, March, 1954.

2. Dale, T. P. and Gladstone, I. H., Phil Trans 153, 317, (1863).

3. Eckert, E. R. G., Introduction to the Transfer of Heat and Mass, McGraw-Hill Book Company, New York, 1950.

4. Hardy, A. C. and Perrin, F. H., The Principles of Optics, McGraw-Hill Book Company, New York, 1932.

5. Jakob, Max, Heat Transfer, John Wiley and Sons, Inc., New York, 1949.

6. Liepmann, H. W., "Deflection and Diffusion of a Light Ray Passing Through a Boundary Layer", Report SM-14397, Douglas Aircraft Co., Santa Monica Division, May, 1952.

7. Moyle, M. P. and Cullen R. E., "Preliminary Investigation of the Heat Requirements for Maintaining Fog Free Photographic Windows on the McDonnell R. F. 101", Internal Report, University of Michigan, Aircraft Propulsion Laboratory, May, 1954.

8. Moyle, M. P., Little, F. K., and Cullen, R. E., "A Review of Aircraft Photographic Systems", Engineering Research Institute, Project 2197, University of Michigan, July, 1954.

9. Moyle, M. P., Little, F. K., and Cullen, R. E., "Thermodynamic Evaluation of the Installation of Electrically Conductive Coated Photographic Windows on the McDonnell R. F. 101", Engineering Research Institute, Project 2197, University of Michigan, September, 1954.

10. Schuh, H., "The Solution of the Laminar Boundary Layer Equations for the Flat Plate for Velocity and Temperature Fields for Variable Properties and for the Diffusion Field at High Concentrations", NACA TN1275, May, 1950.

11. Summary Technical Report of NDRC Volume 1, "Optical Instruments", Washington, D. C., 1946.

12. Wright Field Report on Window Conference, "Photo Reconnaissance File on Defrosting of Camera Windows," July, 1953.

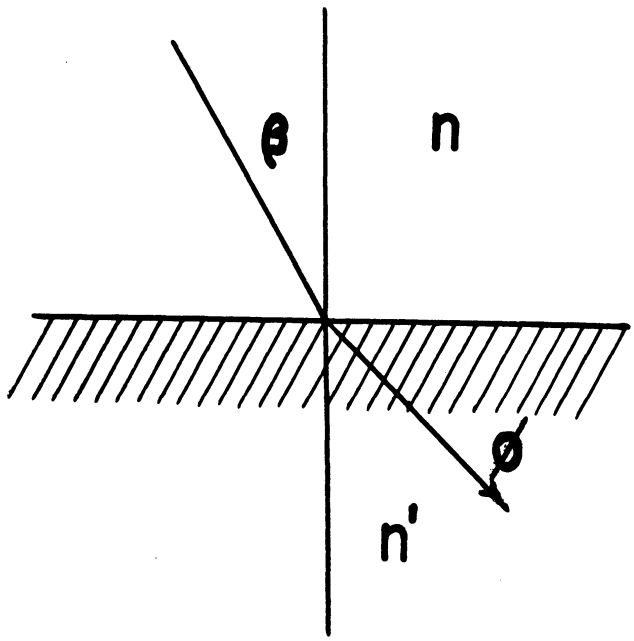

Fig. 1. Bending of ray upon entering a media of different density.

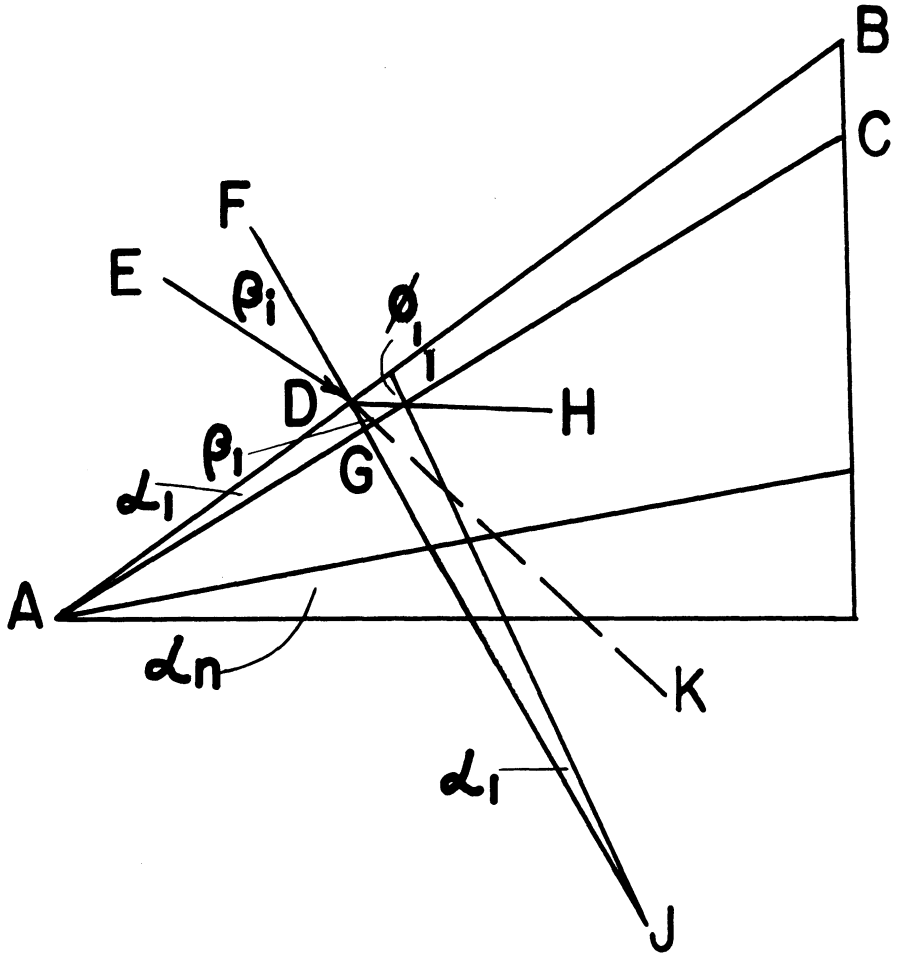

Fig. 2. Angle ray from the first step makes with the perpendicular to the second step.

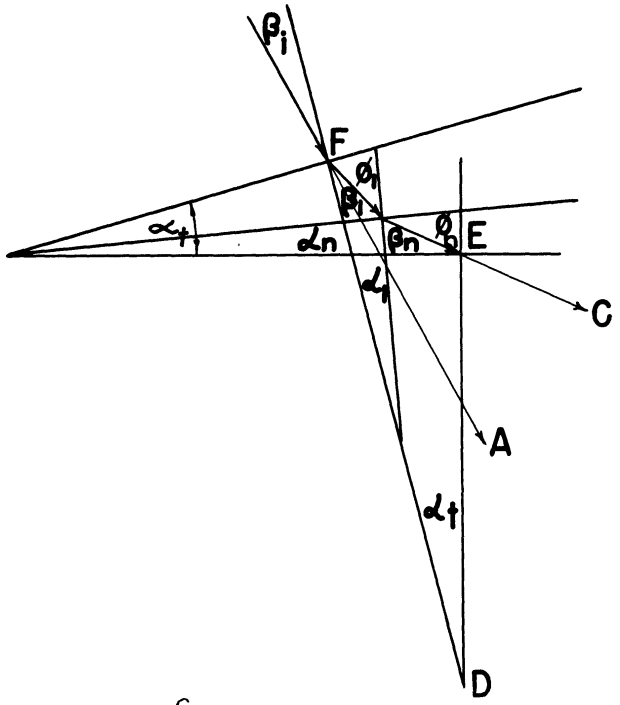

Fig. 3. Total deviation δ a ray makes upon passing through thermal boundary layer.

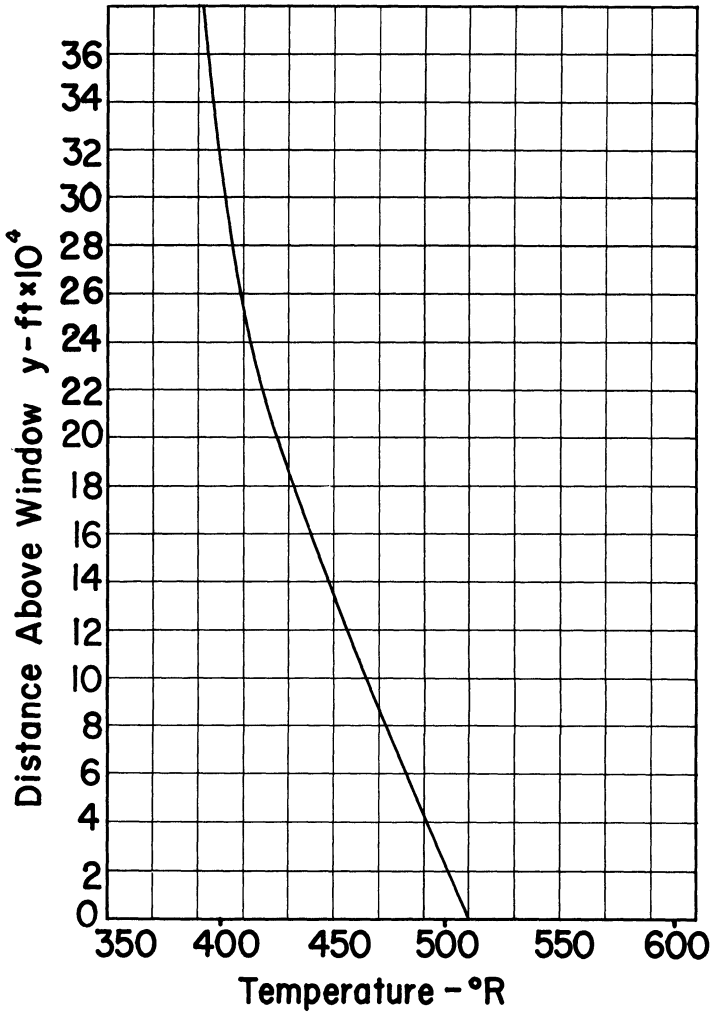

Fig. 4. Temperature profile through boundary layer at center of 12-inch window.

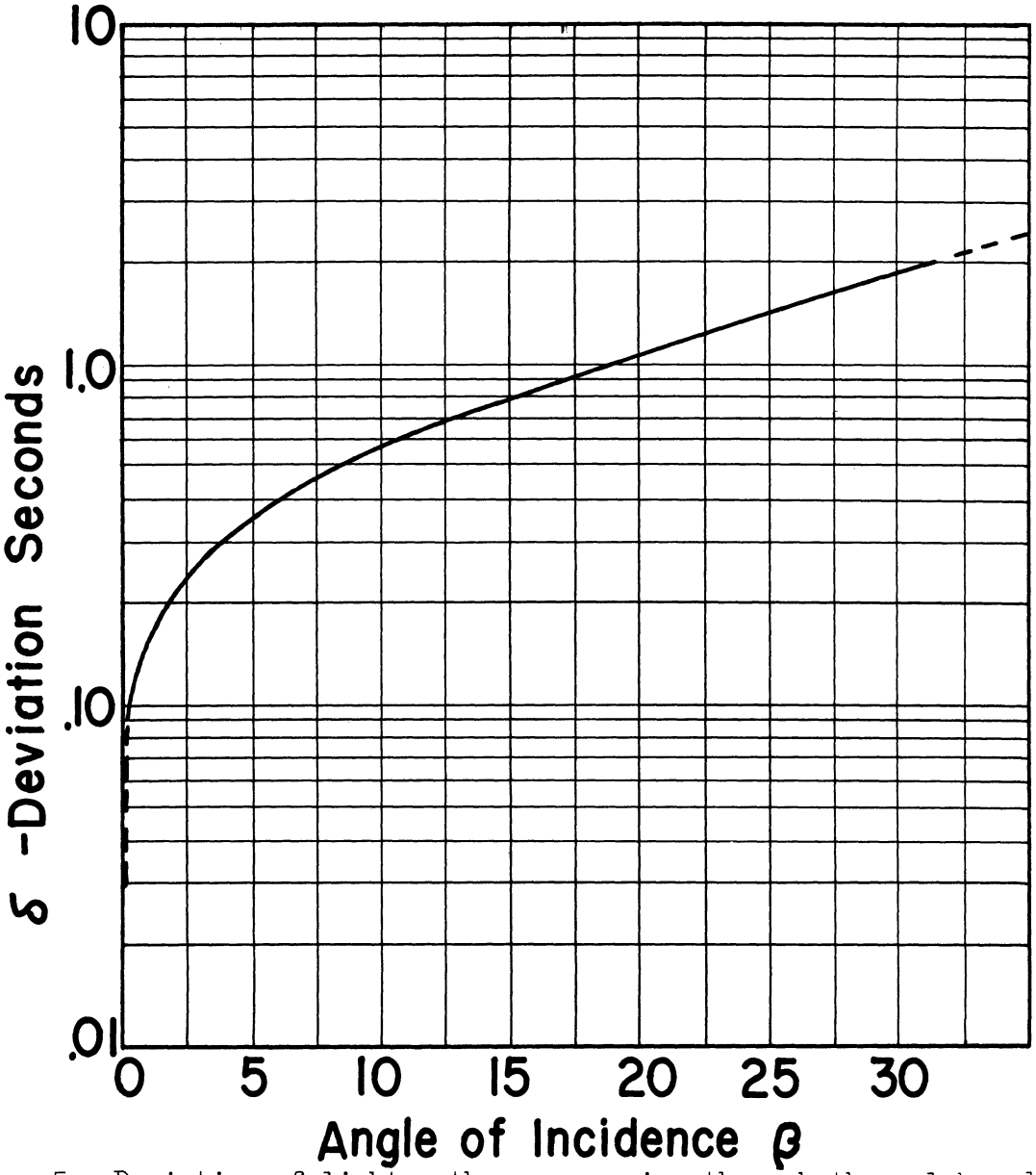

Fig. 5. Deviation of light path upon passing through thermal boundary layer as function of incidence.

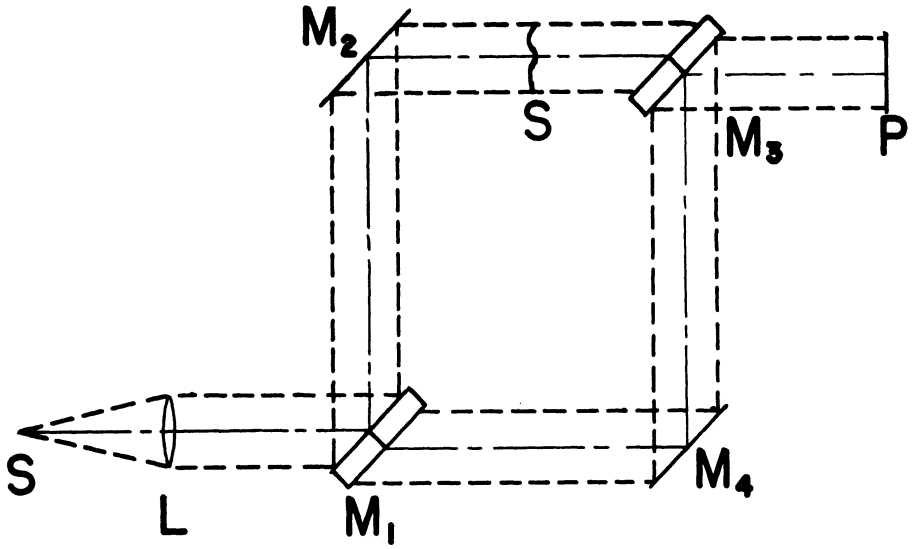

Fig. 6. Optical arrangement of the Mach-Zehnder interferometer.

(a) Unheated Field

(b) 20 Volts Applied 5 Minutes

(c) 40 Volts Applied 5 Minutes

Fig. 7. Intermferometric pictures of the temperature field in the vicinity of a heated photographic window coated with the Liberty-81E electrically conductive coating.

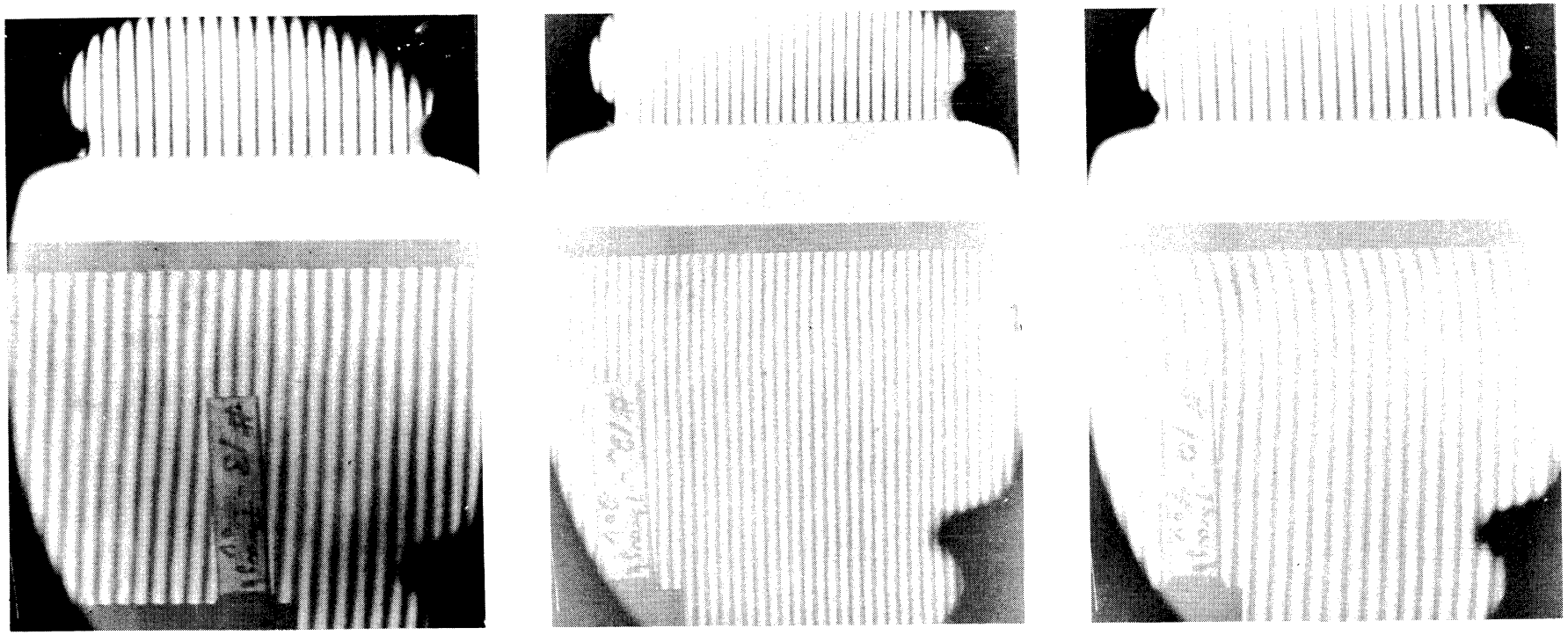

(a) Unheated Field

(b) 20 Volts Applied 5 Minutes

(c) 40 Volts Applied 5 Minutes

Fig. 8. Interferometric pictures of the optical quality of a photographic window coated with the Liberty-81E electrically conductive coating.